Analytical Methods

Accepted Manuscript

This article can be cited before page numbers have been issued, to do this please use: S. Pakrashy, M. Das, S. Manna, S. M. Choudhury, H. Shinziya, B. Das, M. Dolai and A. K. Das, *Anal. Methods*, 2025, DOI: 10.1039/D5AY00778J.

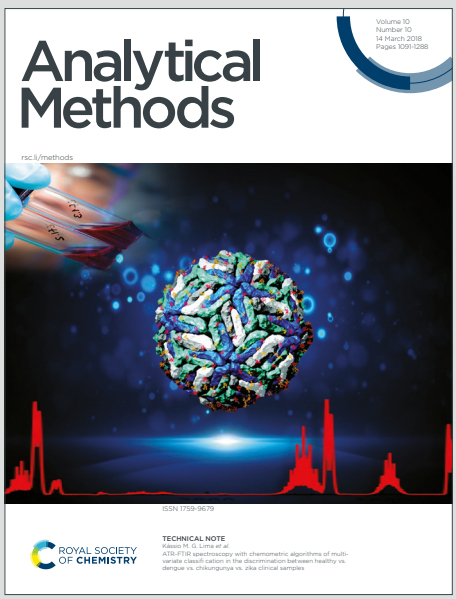

View Article Online
DOI: 10.1039/D5AY00778J

Development of a Natural Product-Based Selective Fluorescent Sensor for Cu^{2+} and DNA/Protein: Insights from Docking, DFT, Cellular Imaging and Anticancer activity

Sourav Pakrashy[a‡], Manik Das[a‡], Sounik Manna[b], Sujata Maiti Choudhury[b], Hazeena Shinziya[c], Bhriguram Das[d], Malay Dolai[a*] and Avijit Kumar Das[c*]

[a] Department of Chemistry, Prabhat Kumar College, Purba Medinipur 721404, W.B., India.
E-mail-dolaimalay@yahoo.in
[b] Biochemistry, Molecular Endocrinology, and Reproductive Physiology Laboratory, Department of Human Physiology, Vidyasagar University, Midnapore721102, W.B., India.
[c] Department of Chemistry, Christ University, Hosur Road, Bangalore, Karnataka, 560029 India, Email: avijitkumar.das@christuniversity.in
[d] Department of Chemistry, Vidyasagar University, Paschim Medinipur 721102, W. B., India.

‡ *Authors are contributed equally*

Abstract

The natural product Seselin (**SS**), was synthesized and characterized spectroscopically for the selective detection of Cu^{2+} and biomolecules such as ct DNA and BSA. The probe exhibits strong bluish emission in a MeOH-H_2O (7:3, v/v) HEPES buffer solution (pH 7.4) at 453 nm. Upon exposure to Cu^{2+}, the **SS** solution shows a selective fluorescence 'turn-off' with a binding constant of 2.13×10^5 M^{-1} and a detection limit of 3.48×10^{-8} M. The HOMO-LUMO energy gap of the probe **SS** decreases from $\Delta E = 7.97$ eV to $\Delta E = 7.77$ eV upon binding with Cu^{2+}, indicating enhanced stability due to ligand-metal complex formation. Significantly, the ligand **SS** exhibits fluorescence enhancement in the presence of ct DNA and BSA, resulting in a visible fluorescence change from colorless to blue, with binding constants of 4.8×10^4 M^{-1} and 4.7×10^4 M^{-1}, respectively. The binding interactions of **SS** with biomacromolecules have been explored through molecular docking studies, revealing that the probe can serve as a promising anti-cancer and anti-viral agent. Furthermore, the probe **SS** demonstrates potent anticancer activity in treatments involving MCF-7 and HLC cells. Additionally, the probe **SS** is capable of detecting intracellular Cu^{2+} in live MCF-7 cell lines.

Keywords: Natural product; Seselin; Copper; Biomolecules; Fluorescence; DFT and docking

View Article Online
DOI: 10.1039/D5AY00778J

1. Introduction

Polyphenols are secondary metabolites with wide distribution in the plant kingdom. Heterocyclic polyphenols hold significant importance in chemistry due to their diverse applications in drug development, photochemistry, agrochemicals, dyes, and more.[1] Notably, the pyranocoumarin framework stands out as a highly promising heterocyclic structure present in both natural and synthetic compounds. It exhibits a wide range of biological activities, including anti-inflammatory, anti-HIV, antitubercular, anti-HBV, anti-dyslipidemic, antiplatelet, antioxidant, and antibacterial properties.[2-4] Seselin, a pyranocoumarin, has been isolated from roots of shamouti orange, sour orange, sweet lime and grapefruit.[5] Seselin significantly influences root development by inhibiting radicle growth in cucumber, lettuce, radish, and wheat seedlings cultivated in darkness.[6] Seselin exhibits DNA-damaging properties and demonstrates cytotoxic effects against various cell lines, including Vero monkey cells, L1210 murine leukemia, CEM leukemia, SW1573 lung tumor, and P-388 lymphocytic leukemia.[7-9] Naturally occurring seselin-type coumarins, such as anomalin, have been shown to suppress skin tumor promotion and counteract the TNF-β-induced reduction in L929 cell viability.[10] However, the chemosensing applicability of Seselin is not disclosed exclusively. Out of different method available for chemosensing behavior, the fluorimetric method is known as versatile to the researcher due to its several advantages like operational simplicity, low cost, super sensitivity etc. However, only a small percentage of fluorescent probes are made directly from natural sources; most are made through an organic reaction with certain hazardous chemicals and a laborious procedure.[11] Once more, compared to synthetic dyes, natural dyes have superior biodegradability, renewable resources, and environmentally favourable qualities.[12-13]

In this context, selective detection of analytes like Cu^{2+} as cations by seselin is very much important and copper is an important cation in biological processes in plant as well as in animals. It is the constituent of different enzyme, protein, vitamin required for mammalian. The excess and deficiency of Cu^{2+} may cause various health issues.[14] Copper is the third most abundant soft transition metal in the human body, following iron and zinc. In a healthy adult, the total copper content is approximately 80 mg, with the highest levels present in the liver and brain. As an essential trace element for higher plants and animals, copper plays a vital role in numerous physiological processes, including iron and zinc metabolism, free radical

View Article Online
DOI: 10.1039/D5AY00778J

elimination, bone development, and the production of skin and hair pigments. An imbalance in copper levels, whether deficiency or excess, can lead to diseases such as Menkes disease, Wilson's disease, and cancer.[15] Therefore, accurate monitoring and detection of Cu^{2+} levels are crucial. Although many chemosensors and chemodosimeters for Cu(II) have been developed, limitations remain, including complex synthesis, high detection limits, dependence on organic solvents, and interference from coexisting transition metals with similar reactivity.[16-18] Although different synthetic material and method were designed and reported for Cu^{2+} sensing, the report of use of natural product-based phytochemicals for selective detection of copper ion is relatively rare (Table S1, ESI).

Furthermore, molecular docking is powerful computational technique that's a key tool in drug discovery and structural molecular biology.[19-20] Molecular docking is a computational technique used to model the interaction between small molecules and proteins at the atomic level. This approach helps in understanding the behavior of small molecules within the binding site of target proteins and provides insights into fundamental biochemical processes.[21-22] The docking can help save time and money in the drug development process, determine the structure of proteins with unknown structures, study protein interactions, drug discovery, predict side effect, biodegradation, can help understand how enzymes work and how they interact with ligands.[23-27] **SS** can disturb the activity of Src, GSK-3β, and ERK cancer cells, cooperate with cisplatin to mark the phosphorylation of p53 in cells, and then stimulate the activity of caspase-3 in cells and cause cell death.[28] In this work, we performed docking study of SS with DNA and protein. Seselin alleviated sepsis induced by caecal ligation and puncture, reducing pro-inflammatory factor levels and inhibiting STAT1 and p6 activity. Its anti-inflammatory effects are attributed to its modulation of Jak2 activity.[29] Therefore, we have utilized the usefulness of phytochemical **SS** for the detection of copper and DNA/protein in solution as well as in live cell along with the docking studies to get its more exploration. The phytochemical **SS** has been characterized by ^{1}H NMR and mass spectra (Fig.S1-S3).

View Article Online
DOI: 10.1039/D5AY00778J

2. Experimental Section

2.1 Material and Methods

The materials and the methods of study are described in the supporting file. The detailed photophysical studies (solution preparation, fluorescence study, binding constant determination[30-31], detection limit [32] etc.,) DFT calculations [33-41], Molecular docking [19,21,42-44] and bio-imaging[32,45,46] were described in the supporting information.

2.2 Synthesis of Seselin (SS)

The total synthesis of seselin was carried out in two steps as shown in Scheme 1.

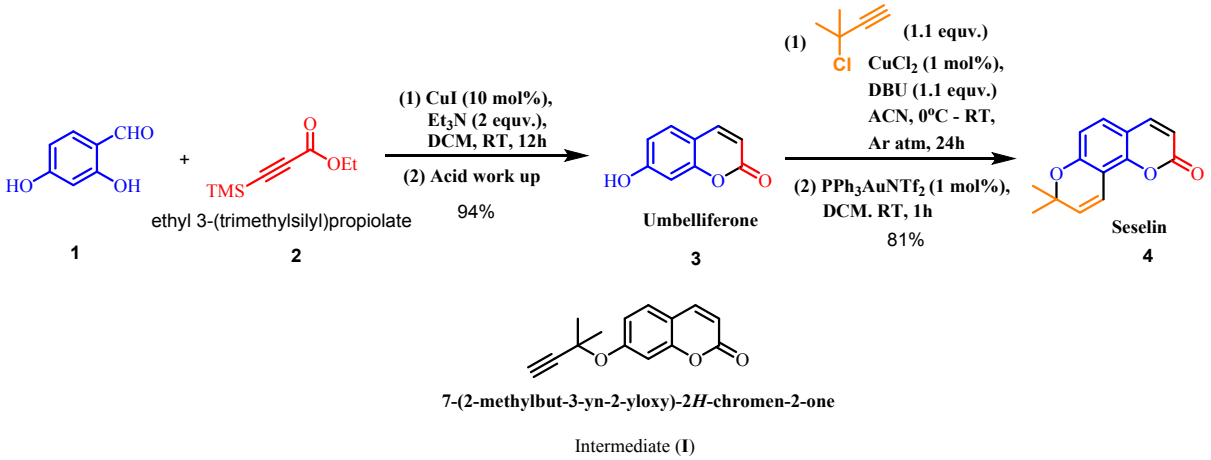

Scheme 1: Total Synthesis of Seselin

Synthesis of Umbelliferone (3): 4-hydroxy salicylaldehyde (1) [0.5 mmol], Ethyl 3-(trimethylsilyl) propiolate (2) [0.5 mmol] and CuI [0.05 mmol] were taken in a clean and dry 10 ml round bottom flask. Then, dichloromethane [3 ml] was added to it under stirring and followed by Et_3N [1.0 mmol] addition. The reaction was kept in stirring overnight. After completion of the reaction (confirmed by TLC monitoring), the reaction was quenched with 1(N) HCl and then worked up and combined organic layer was washed with brine solution and eventually that was extracted with DCM. Umbelliferone was purified by column chromatography with (1:7) ethyl acetate in petroleum ether as eluent (Yield: 94%). **^{1}H NMR (DMSO-d_6, 400 MHz): δ (ppm)**: 6.13 (1H, d), 6.68 (1H, d), 6.76 (1H, s), 7.47 (1H, d), 7.87 (1H, d), 10.47 (1H).

View Article Online
DOI: 10.1039/D5AY00778J

Synthesis of Seselin (4): Umbelliferon (3) [0.3 mmol] and 3-chloro-3-methylbut-1-yne [0.33 mmol] were taken in a clean and oven-dried 10 ml reaction vial along with $CuCl_2$ [0.003 mmol] as catalyst and DBU [0.33 mmol] as base in acetonitrile solvent at ice-bath temperature initially to ambient temperature under argon atmosphere for 24h to get the substitution product intermediate I. Then, the intermediate I without purification was treated with $Ph_3PAuNTf_2$ [0.003 mmol] as the catalyst for eventual annulation in dichloromethane at room temperature for an hour under same reaction pot (after evaporation of the acetonitrile solvent) to obtain the target product Seselin (4) after work up with dichloromethane. Seselin was purified by column chromatography with (1:10) ethyl acetate in petroleum ether as eluent (Yield: 81 %). The melting point was found in open capillary tubes in a Köfler block apparatus at 119.6 ºC.

^{1}H NMR ($CDCl_3$, 400 MHz): δ (ppm): 1.49 (6H, s), 5.7 (1H, d), 6.2 (1H, d), 6.7 (1H, d), 6.9 (1H, d), 7.2 (1H, d), 7.63 (1H, d). ESI-MS: 229.0 (found), 228.07 (calcd.). **^{13}C NMR ($CDCl_3$, 100 MHz): δ (ppm)**: 161.11, 156.33, 150.12, 143.96, 130.79, 127.79, 115.02, 113.56, 112.63, 109.32, 28.14

3. Results and discussion

3.1 Spectroscopic Response of SS towards several cations

Spectroscopically to check the sensing behavior of the probe **SS** towards several cations, fluorescence spectra of **SS** (5×10^{-6} M) was recorded in the presence of different metal ions in MeOH – HEPES buffer (7:3 v/v). The probe exhibits high fluorescence near at 453 nm (ϕ = 0.197) upon excitation at λ_{ex} = 330 nm (Fig. 1). Before continuing the sensing process, the pH stability of the probe as well as its stability in the working buffer solution were investigated for its biomedical application purpose. In this context, the emission change of **SS** was separately recorded by varying the pH of the solvent (pH = 2 – 12). The result shows that it is highly emissive in neutral pH or even in slightly high pH solutions having the highest emission capabilities (Fig. S4). The fluorescence spectra were recorded with time and it has been observed that there is a minimal change in the fluorescence spectra of the probe, indicating that it is stable in the working buffer media (Fig. S5). After standardizing the pH of the buffer, the fluorescence spectra were recorded in MeOH –HEPES buffer media (7:3 v/v)

View Article Online
DOI: 10.1039/D5AY00778J

at pH 7.4. Herein, it was observed that among several cations, only in the presence of Cu(II) ion, the fluorescence intensity of the probe was quenched while other cations did not make any significant change in the fluorescence response of the probe (Fig.1). This result suggests that the natural product **SS** can act as a selective sensor for Cu^{2+}.

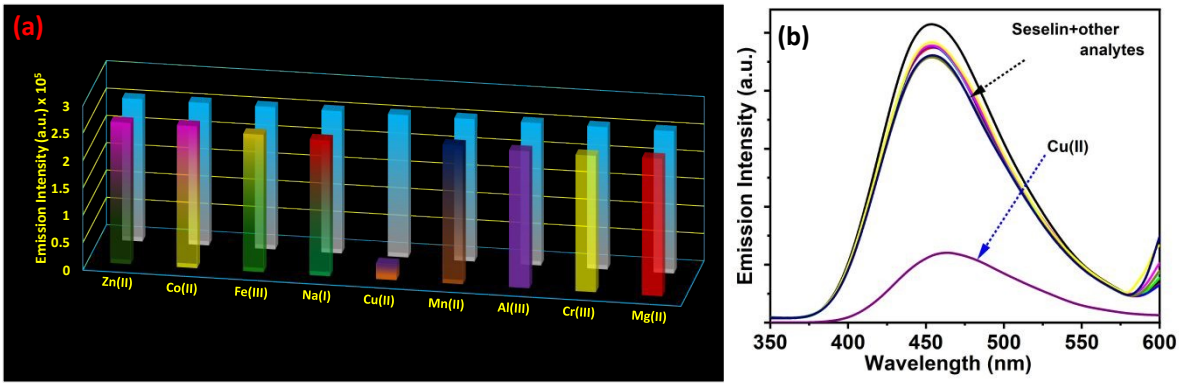

Figure 1(a) Change of emission intensity of **SS** (5×10^{-6} M) in the presence of various interfering metal ions (2×10^{-5} M). (b) corresponding fluorescence spectra in MeOH – H_2O (7:3, v/v) HEPES buffer media at pH 7.4 upon excitation at 330 nm.

In the UV–vis spectroscopic analysis of **SS** (5×10^{-6} M) with Cu^{2+} (2×10^{-5} M) in a MeOH–H_2O (7:3, v/v) HEPES buffer solution at pH 7.4, a pronounced ligand absorption peak at 330 nm gradually decreased upon incremental addition of Cu^{2+} ions. Concurrently, a red-shifted absorption band emerged at 400 nm, accompanied by a distinct isosbestic point at 370 nm (Fig.S7). These significant spectral changes, particularly the red-shifted band, suggest strong interaction between **SS** and Cu^{2+} ions.

Fluorescent titration of SS with Cu (II)

To demonstrate the sensitivity of **SS** with Cu (II), fluorescence study was performed at a fixed concentration of the probe **SS** (5×10^{-6} M) in MeOH – HEPES buffer solution (7:3, v/v). Initially **SS** originates strong fluorescence due to its conjugated π-electron system, which spans the fused coumarin and furan rings. Moreover, the rigid planar structure of seselin reduces non-radiative decay pathways, enhancing the emission intensity at 453 nm. Additionally, the presence of electron-donating and withdrawing groups on the coumarin moiety can influence the photophysical behavior by modulating the energy gap between the

View Article Online
DOI: 10.1039/D5AY00778J

excited and ground states. From the titration profiles, it has been observed that upon incremental addition of Cu (II) (1 – 25 μM) to the ligand solution, the fluorescence intensity at 453 nm was gradually diminished with a red shift of the emission maxima ($\Delta\lambda$ = 10 nm) (Fig. 2a). The Cu^{2+} ion has an open shell d^9 electronic structure and exhibit notable quenching response on binding with **SS** due to the chelation enhanced quenching (CHEQ) effect.[47,48] The ligand **SS** and Cu^{2+} complex formation was confirmed by the appearance of a mass peak at m/z = 393 (calculated mass: 392.97) (Fig.S9), corresponding to [Cu(**SS**)$(Cl)_2$(MeOH)] ensemble (scheme 2). From the titration plot of emission intensity vs metal concentration, the detection limit (LOD) of **SS** towards Cu(II) was calculated as 3.48×10^{-8} M (Fig. 2b). From linear fitting and the intercept of the titration plot, the binding constant was calculated as 2.13×10^5 M^{-1} (Fig. S10) and through the Jobs plot analysis, the 1:1 binding stoichiometry for **SS**–Cu^{2+} complexation was verified (Fig.S8).

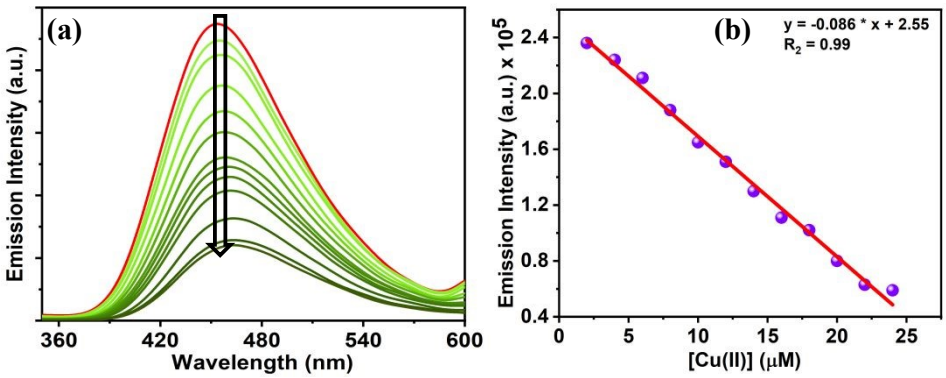

Figure 2 (a) Change of Emission intensity of **SS** (5×10^{-6} M) after incremental addition of Cu(II)(1 – 25 μM) in MeOH – H_2O (7:3 v/v) HEPES buffer solution at pH 7.4. (b) Determination of LOD value of **SS** for Cu(II) ion.

3.2 Reversibility and Interference Performance

Reversibility and reproducibility are crucial attributes for sensors, offering significant advantages for sustainable research and practical applications. During sensing of the Cu(II), the reversibility of **SS** can be achieved by the alternative addition of Cu(II) ion and ethylene diamine tetra acetate (EDTA) into **SS** – Cu(II) complex solution. Here EDTA acts as a

View Article Online
DOI: 10.1039/D5AY00778D

masking agent for Cu(II). From the experimental result it has been observed that this reversible cycle can be performed up to 10 times with marked contrast of the emission intensity alternation (Fig. 3a).

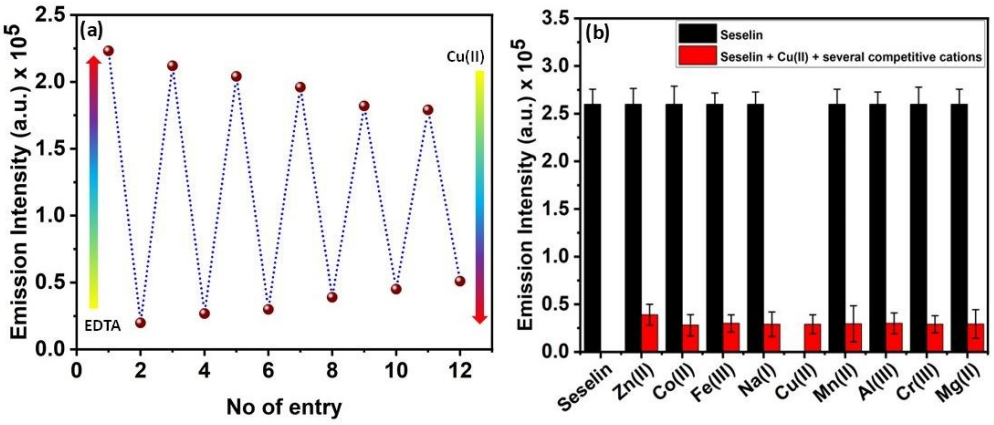

Figure 3 (a) Reversibility experiment of **SS** by alternative addition of Cu(II) and EDTA in MeOH – H_2O (7:3 v/v) HEPES buffer solution. (b) Change of Emission intensity of **SS** – Cu(II) conjugate in the presence of several competitive cations in MeOH – H_2O (7:3 v/v) HEPES buffer solution.

To explain the interference by other competitive cations during the sensing of Cu(II), emission spectra of **SS** – Cu(II) complex in presence of several competitive cations has been measured and there is no significant interference by any other metal ions on binding of **SS** with Cu(II) (Fig. 3b).

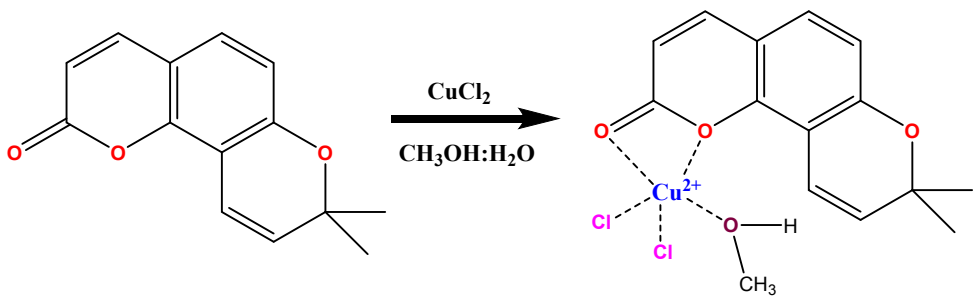

Scheme 2 Probable binding mode of **SS** with Cu^{2+} complex in methanol water medium.

3.4 Geometry optimization and electronic structure

The optimized geometries of probe **SS** and its Cu(II) complex are depicted in Fig. 4a. HRMS data confirmed the composition of the complex as [Cu(**SS**)$(Cl)_2$(MeOH)](**1**), which was

View Article Online
DOI: 10.1039/D5AY00778J

subsequently subjected to theoretical geometry optimization using DFT/B3LYP methods. The positive and negative phases are illustrated in orange and blue, respectively.

The metal center Cu^{2+} is being penta-coordinated in complex **1** with neutral bi-dentate ligand (L) (with O_2 donor sites), two Cl^- ion and one MeOH as solvents to attain the arrangement of distorted square pyramidal geometry to form **[Cu(SS)(Cl)$_2$(MeOH)] (1)**. The calculated Cu–O and Cu-Cl bond distances are fall in the range 1.94-2.11Å and 2.11-2.12Å respectively. Interestingly, it has been observed that the formation of monomer complex with probe **SS**, the HOMO-LUMO energy gap (ΔE = 7.77 eV for **1**) decreases from that of the bare probe (ΔE=7.97 eV) (Fig. 4b).

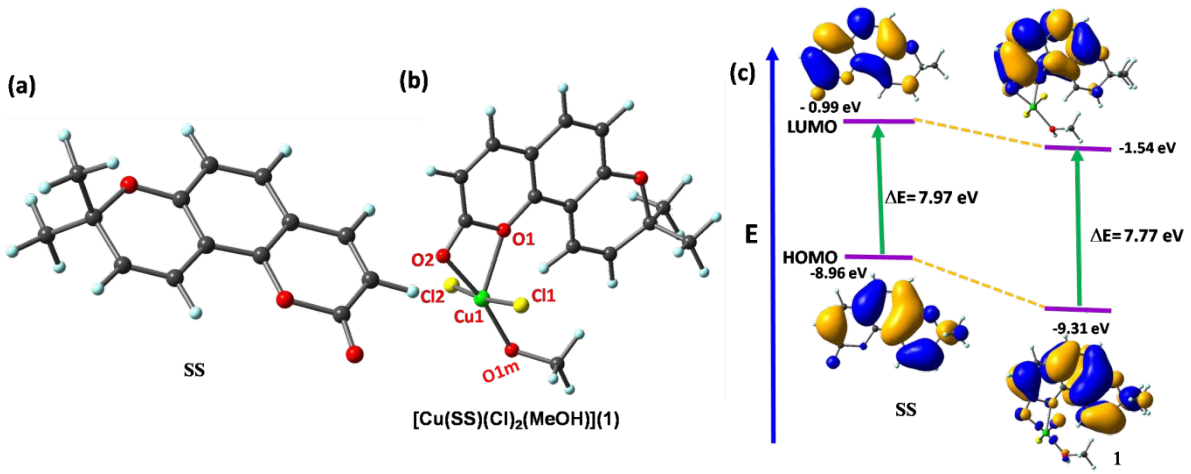

Figure 4: Geometry optimized molecular structure of (a) **SS** (L) and (b) **[Cu(L)(Cl)$_2$(MeOH)]$^{2+}$(1)**; (c) Frontier molecular orbitals of **SS** and **1**.

3.5 Fluorometric binding study of SS with DNA and protein BSA

The fluorescence experiments of **SS** with DNA/protein have been performed in Tris-HCl buffer at pH = 7.2. In the emission spectra, **SS** showed a weak emission signal at 462 nm (λ_{ex} = 330 nm) in the absence of ct DNA and BSA. However, the increasing concentration of ct DNA and BSA in the **SS** solution led to the significant fluorescence enhancement at 460 nm and 458 nm respectively (Fig. 5 and Fig. 6). The detection limits of **SS** for ct DNA and BSA from fluorescence measurements are 1.05μM and 0.0024μM respectively (Fig. S11). The binding constants of **SS** with ct DNA and BSA obtained from non-linear fitting curves from spectrofluorometric titrations are 4.8 × 10^4 M^{-1} and 4.7 × 10^4 M^{-1} respectively (Fig. S12).

View Article Online
DOI: 10.1039/D5AY00778J

The enhancement of the fluorescence response of **SS** on binding with ct DNA and BSA is due to the polarity of the binding cavities and the CS or ICT state of **SS** is stabilized more proficiently inside the more polar DNA and protein binding cavity.[49] The details interaction pathways of **SS** with DNA and proteins have been explained through molecular docking analysis.

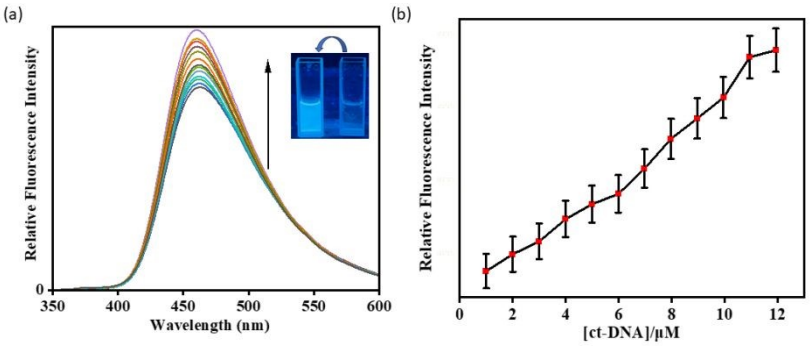

Figure 5. Fluorescence titration of **SS** (c = 2.0 × 10^{-5} M) upon incremental addition of ct-DNA (c = 2 mM) in Tris-HCl buffer, pH = 7.2.

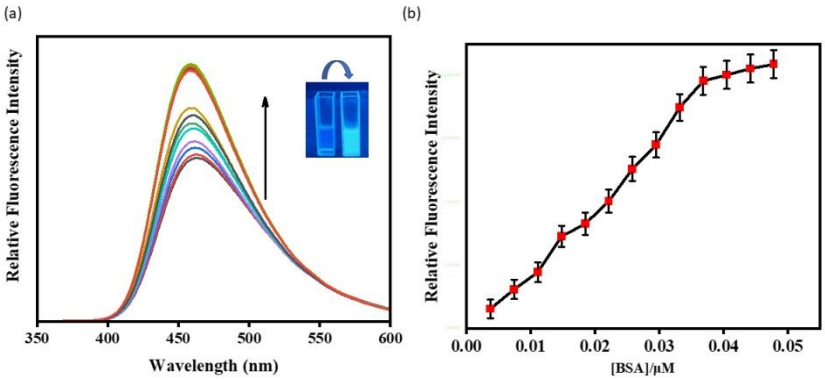

Figure 6. Fluorescence titration of **SS** (c = 2.0 × 10^{-5} M) upon incremental addition of BSA protein (c = 7.4μM) in Tris-HCl buffer, pH = 7.2.

3.6 Docking Study of SS with Biomacromolecules

The BSA proteins PDB-ID: 6QS9 (Bovine Serum Albumin in complex with Ketoprofen) and 4OR0 (Crystal Structure of Bovine Serum Albumin in complex with naproxen) docking with **SS** showed strong binding. The calculations reveal the maximum free energy change for these interactions as ΔG = -8.7, and -9.4 Kcal/mol (Table 1).

View Article Online
DOI: 10.1039/D5AY00778J

The binding energy between **SS** with CT-DNA (PDB-ID: 1BNA) from docking calculation reveals the maximum free energy change for the interaction is ΔG = -7.4 Kcal/mol (Table 2).

Table 1: Results of **SS** docking with proteins

Name of targeted proteins	**PDB ID**	**Docking score (Kcal/mol)**
		SS
BSA in complex with Ketoprofen	6QS9	-8.7
BSA in complex with naproxen	4OR0	-9.4

Table 2: Results of **SS** docking with DNA

Name of targeted DNAs	**PDB ID**	**Docking score (Kcal/mol)**
		SS
STRUCTURE OF A B-DNA DODECAMER	1BNA	-7.4

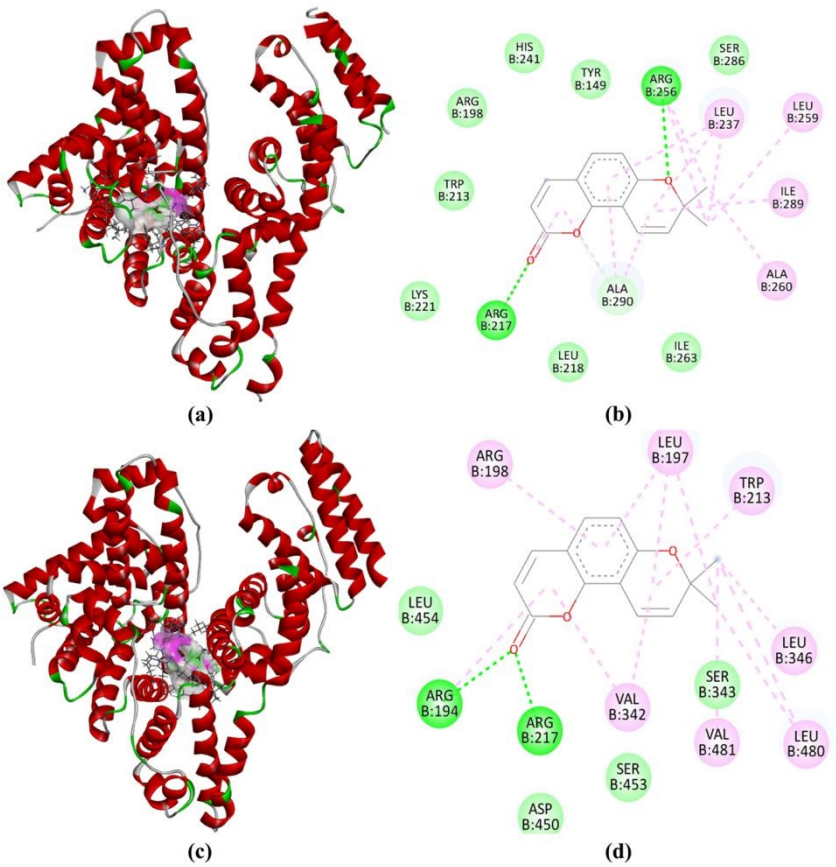

View Article Online
DOI: 10.1039/D5AY00778J

Figure 7 (a) Pictorial observation of the docked **SS** inside the active site of the 6QS9, with an engrossed (b) 2D interpretation of its interaction with binding site amino acid residues. (c) Pictorial observation of the docked **SS** inside the active site of the 4OR0, with an engrossed (d) 2D interpretation of its interaction with binding site amino acid residues.

Fig. 7a represents the docked **SS** at the active site of 6SQ9 with two hydrogen bonding between the ligand and 217th and 256th ARG residue of chain B (Fig. 7b), and Fig. 7c represents the docked **SS** at the active site of 4OR0 with two hydrogen bonding between the ligand and 194th and 217th ARG residue of chain B (Fig. 7d).

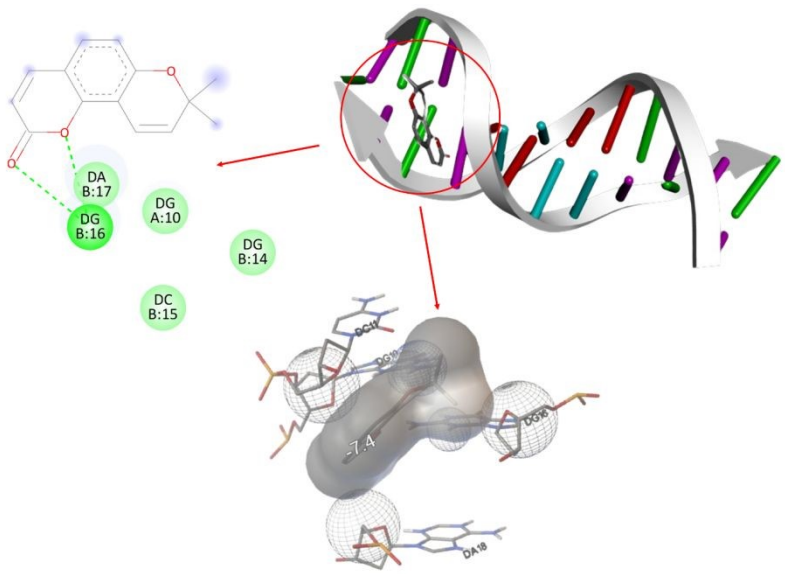

Figure 8 Pictorial observation of the docked **SS** inside the active site of the DNA 1BNA binding protein, with an engrossed understanding of its interaction with nucleotides.

Fig. 8 reveals the binding of the docked **SS** with B-DNA Dodecamer (1BNA), showing the hydrogen bond interaction with 16thDG residue of chain B. Thus, the docking results with these bio-macromolecules predict that it has good binding properties and can be embraced as potent inhibitor for the development of new cancer treatment drugs.

3.7 Anticancer activity of SS and biosensor imaging

View Article Online
DOI: 10.1039/D5AY00778J

The docking study shows the probe have good anti-cancer activity. To verify this prediction, the cytotoxicity was conducted experimentally using the MCF 7 and HLCs cell lines according to standard protocol. Moreover, *in-vitro* cell imaging study with **SS** was also performed to explore the biological utility of the probe for Cu^{2+}.

3.7.1 Cell viability study on MCF 7 and human lymphocyte cells (HLCs)

The cytotoxicity of **SS** against MCF-7 cells was assessed using the MTT assay. The results demonstrated that **SS** significantly reduced cell viability in a dose-dependent manner showing strong cytotoxic activity against these cells. The IC_{50} value of **SS** was found to be 23.17 µg/mL, which is comparable to the IC_{50} value of the standard anticancer drug 5-FU (16.14 µg/mL), demonstrating that **SS** also has a cytotoxic effect (Fig. 9a). Time-dependent cell viability study exhibited that SS inhibited cell viability 53.87% and 40.16 %, at 24h and 48h, respectively (Fig. 9b). These findings clearly demonstrate the cytotoxic potential of SS against MCF-7 cells. Furthermore, **SS** did not exhibit significant toxicity to lymphocytes at doses up to 50 µg/mL, with only a slight reduction in lymphocyte viability observed (Fig. 9c). These findings suggest that SS could be a potent anticancer agent for use in treatments involving MCF-7 cells.

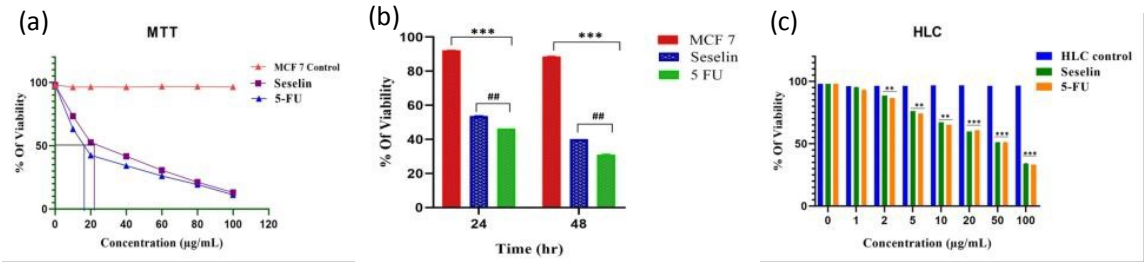

Figure 9 (a) The cytotoxic effect of SS on MCF-7 cells was evaluated at different concentrations. (b) Cell viability was assessed at 24- and 48-hours following treatment with SS, and the IC50 value was determined. Results are presented as Mean ± SEM (n = 3); ***p < 0.001, #p < 0.05, ##p < 0.01, ###p < 0.001; * compared with the control, # compared with 5-FU. (c) A minimal reduction in lymphocyte viability was observed at SS concentrations as high as 50 µg ml^{-1}. Data are expressed as Mean ± SEM from three independent experiments; **p < 0.01, ***p < 0.001 compared to the control group.

View Article Online
DOI: 10.1039/D5AY00778J

3.7.2 Bio-imaging study

During one-hour incubation at 37°C with **SS** at its IC_{50} concentration, intense intracellular blue fluorescence was detected, indicating high intensity of **SS** inside the cells. However, when cells were incubated with an external Cu^{2+} ion solution, no notable intracellular emission has been observed. **SS** easily penetrated the cell membrane and showed blue fluorescence but when **SS** with Cu^{2+} ions based on the fluorescence images, which did not show significant blue fluorescence for the development of **SS**-Cu^{2+} complex (Fig 10). These findings suggest that **SS** could act as a selective sensor for detecting Cu^{2+} ions in bio-imaging at specific concentrations and incubation times.

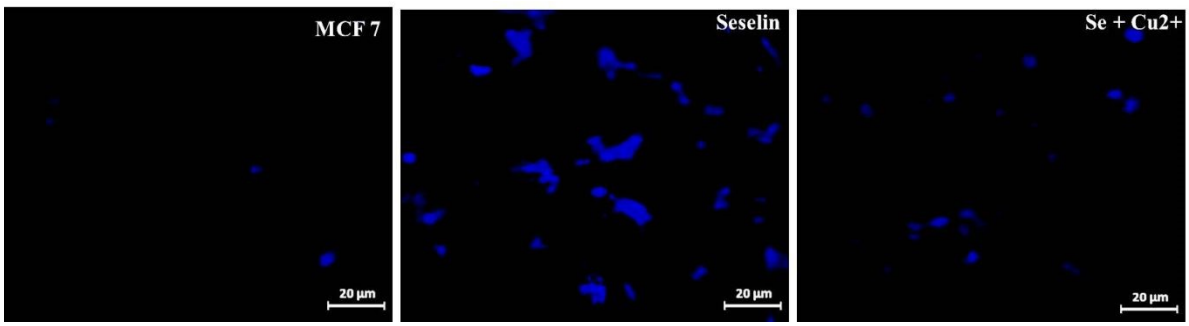

Figure 10 Intercellular biosensor cell imaging study was observed on MCF7 cells. Cells were incubated alone with free **SS** and brighter blue fluorescence was observed other than **SS** + Cu^{2+} treated groups.

4. Conclusion

The natural product Seselin (**SS**) was synthesized and characterized spectroscopically, exhibiting strong bluish emission at 453 nm. In the presence of Cu^{2+}, the probe solution showed a turn-off sensing phenomenon among various cations, with the binding constant and detection limit determined to be 2.13×10^5 M^{-1} and 6.97×10^{-8} M, respectively. DFT calculations revealed that the binding of Cu^{2+} with **SS** decreases the HOMO-LUMO energy gap from $\Delta E = 7.97$ eV to $\Delta E = 7.77$ eV, indicating stable complex formation between the ligand and metal. Notably, the ligand **SS** displays fluorescence enhancement in the presence of ct DNA and BSA, resulting in a visible fluorescence change from colorless to blue. The

View Article Online
DOI: 10.1039/D5AY00778J

binding constants were determined to be 4.8×10^4 M^{-1} and 4.7×10^4 M^{-1}, respectively. The probe **SS** also exhibits promising anticancer and antiviral properties, as supported by docking studies with DNA biomacromolecules. Furthermore, the potent anticancer activity of **SS** was confirmed by an MTT assay using MCF-7 and HLC cells. Moreover, the probe **SS** is capable of detecting intracellular Cu^{2+} in live MCF-7 cells.

5. Conflicts of interest

There are no conflicts of interest to declare.

6. Acknowledgements

MD acknowledges to Science & Engineering Research Board (SERB), Govt. of India (ref No.PDF/2016/000334). Avijit Kumar Das specially acknowledges State University Research Excellence (SERB-SURE) of the Science and Engineering Research Board (SERB) (File Number: SUR/2022/ 002461) under Anusandhan National Research Foundation (ANRF) and Department of Science and Technology (DST), Government of India, for the financial support by the research grant.

7. References

1 J. Jampilek, *Molecules*, 2019, 24.

2 C.-R. Su, S. F. Yeh, C. M. Liu, A. G. Damu, T.-H. Kuo, P.-C. Chiang, K. F. Bastow, K.-H. Lee and T.-S. Wu, *Bioorg. Med. Chem.*, 2009, **17**, 6137–6143.

3 F. Salehian, H. Nadri, L. Jalili-Baleh, L. Youseftabar-Miri, S. N. Abbas Bukhari, A. Foroumadi, T. Tüylü Küçükkilinç, M. Sharifzadeh and M. Khoobi, *Eur. J. Med. Chem.*, 2021, **212**, 113034.

4 S. J. Min, H. Lee, M.-S. Shin and J. W. Lee, *Int. J. Mol. Sci.*, 2023, 24.

5 E. Tomer, R. Goren and S. P. Monselise, *Phytochemistry*, 1969, **8**, 1315–1316.

6 E. T. Raphael Goren, *Plant Physiol.*, **Volume 47,** Pages 312–316,.

7 K. Ostrowska, W. Olejarz, M. Wrzosek, A. Głuszko, G. Nowicka, M. Szczepański, I. B. Materek, A. E. Kozioł and M. Struga, *Biomed. Pharmacother.*, 2017, **95**, 1412–1424.

8 F. Nagase, K. Ueda, I. Nakashima, K. Kawashima, K. Isobe, E. Nagura, K. Yamada,

View Article Online
DOI: 10.1039/D5AY00778J

T. Yokochi, Y. Hasegawa and T. Yoshida, *Int. J. cancer*, 1986, **38**, 907–914.

9 J. F. Alhmoud, A. G. Mustafa and M. I. Malki, *Int. J. Mol. Sci.*, , DOI:10.3390/ijms21197365.

10 H. Nishino, T. Okuyama, M. Takata, S. Shibata, H. Tokuda, J. Takayasu, T. Hasegawa, A. Nishino, H. Ueyama and A. Iwashima, *Carcinogenesis*, 1990, **11**, 1557–1561.

11 M. Rajasekar, V. Ranjitha and K. Rajasekar, *Results Chem.*, 2023, **5**, 100850.

12 D.-B. Sung and J. S. Lee, *RSC Med. Chem.*, 2023, **14**, 412–432.

13 S. Yadav, K. S. Tiwari, C. Gupta, M. K. Tiwari, A. Khan and S. P. Sonkar, *Results Chem.*, 2023, **5**, 100733.

14 R. A. Løvstad, *Biometals*, 2004, **17**, 111–113.

15 (a) T. Chopra, S. Sasan, L. Devi, R. Parkesh, and K. K. Kapoor, *Coord. Chem. Rev.*, 2022, **470**, 214704. (c) M. S. Kumar, S. Vishnu, M. Dolai, A. Nag, Y. Bylappa and A. K. Das, *Anal. Methods,* 2024, **16**, 676-685.

16 (a) M. Kumar, N. Kumar, V. Bhalla, P. R. Sharma and T. Kaur, *Org. Lett.*, 2012, **14**, 406–409. (b) S. Goswami, S. Maity, A. C. Maity, A. K. Maity, A. K. Das, P. Saha, *RSC Adv*., 2014, **4**, 6300-6305. (c) S. Goswami, D. Sen, A. K. Das, N. K. Das, K. Aich, H. K. Fun, C. K. Quah, A. K. Maity, P. Saha, *Sensors and Actuators B: Chemical* 2013, **183**, 518-525. (d) S. Goswami, S. Maity, A. K. Das, A. C. Maity, *Tetrahedron Lett*., 2013, **54**, 6631-6634.

17 (a) D. Wu, A. C. Sedgwick, T. Gunnlaugsson, E. U. Akkaya, J. Yoon and T. D. James, *Chem. Soc. Rev.*, 2017, **46**, 7105-7123. (b) S Vishnu, A. Nag, A. K. Das, *Anal. Methods*, 2024,**16**, 5263-5271.

18 (a) S. Liu, Y. M. Wang, J. Han, Journal of Photochemistry and Photobiology C: Photochemistry 2017, **32**, 78-103. (b) S Vishnu, A. K. Das, Y. Bylappa, A. Nag, M. Dolai, *Anal. Methods*, 2024, **16**, 8164-8178.

19 P. C. Agu, C. A. Afiukwa, O. U. Orji, E. M. Ezeh, I. H. Ofoke, C. O. Ogbu, E. I. Ugwuja and P. M. Aja, *Sci. Rep.*, 2023, **13**, 13398.

20 X.-Y. Meng, H.-X. Zhang, M. Mezei and M. Cui, *Curr. Comput. Aided. Drug Des.*, 2011, **7**, 146–157.

21 A. Kukol, *Molecular Modeling of Proteins*, 2008.

View Article Online
DOI: 10.1039/D5AY00778J

22 A. E. Cho, V. Guallar, B. J. Berne and R. Friesner, *J. Comput. Chem.*, 2005, **26**, 915–931.

23 C. Guerrero-Perilla, F. A. Bernal and E. D. Coy-Barrera, *Rev. Colomb. Ciencias Químico-Farmacéuticas*, 2015, **44**, 162–178.

24 G. Sliwoski, S. Kothiwale, J. Meiler, E.W. Lowe, *Pharmacol. Rev*. 2014, **66**, 334–395.

25 L. Pinzi and G. Rastelli, *Int. J. Mol. Sci.*, 2019, 20.

26 L. G. Ferreira, R. N. Dos Santos, G. Oliva and A. D. Andricopulo, *Molecules*, 2015, **20**, 13384–13421.

27 D.B. Kitchen, H. Decornez, J.R. Furr, J. Bajorath, *Nat. Rev. Drug Discov*. 2004, **3**, 935–949.

28 R. Y. Shyu, C. H. Wang, C. C. Wu, L. K. Wang and F. M. Tsai, *Arch. Biol. Sci.*, 2023, **75**, 287–297.

29 L. Feng, Y. Sun, P. Song, L. Xu, X. Wu, X. Wu, Y. Shen, Y. Sun, L. Kong, X. Wu and Q. Xu, *Br. J. Pharmacol.*, 2019, **176**, 317–333.

30 H. A. Benesi and J. H. Hildebrand, *J. Am. Chem. Soc.*, 1949, **71**, 2703–2707.

31 R. Banerjee, R. Sinha and P. Purkayastha, *ACS Omega*, 2019, **4**, 16153–16158.

32 G. C. Das, B. Das, U. Saha, S. Kanta Dey, S. Maiti Choudhury, P. Brandao, A. A. Alothman, S. M. Wabaidur and M. Dolai, *Inorganica Chim. Acta*, 2024, 122404.

33 R. G. Parr, eds. K. Fukui and B. Pullman, Springer Netherlands, Dordrecht, 1980, pp. 5–15.

34 M. Cossi and V. Barone, *J. Chem. Phys.*, 2001, **115**, 4708–4717.

35 M. Cossi, N. Rega, G. Scalmani and V. Barone, *J. Comput. Chem.*, 2003, **24**, 669–681.

36 V. Barone and M. Cossi, *J. Phys. Chem. A*, 1998, **102**, 1995–2001.

37 A. D. Becke, *J. Chem. Phys.*, 1993, **98**, 5648–5652.

38 C. Lee, W. Yang and R. G. Parr, *Phys. Rev. B*, 1988, **37**, 785–789.

39 M. E. Casida, C. Jamorski, K. C. Casida and D. R. Salahub, *J. Chem. Phys.*, 1998, **108**, 4439–4449.

40 M. J. Frisch Trucks, G.W., Schlegel, H.B., Scuseria, G.E., Robb, M.A., Cheeseman, J.R., Scalmani, G., Barone, V., Mennucci, B., Petersson, G.A., Nakatsuji, H., Caricato, M., Li, X., Hratchian, H.P., Izmaylov, A.F., Bloino, J., Zheng, G., Sonnenberg, J.L., Wall, *Gaussian Inc., 2009, Wallingford CT.*, , DOI:10.1007/s11172-018-2377-z.

View Article Online
DOI: 10.1039/D5AY00778J

41 N. M. O'boyle, A. L. Tenderholt and K. M. Langner, *J. Comput. Chem.*, 2008, **29**, 839–845.

42 G. M. Morris and M. Lim-Wilby, ed. A. Kukol, Humana Press, Totowa, NJ, 2008, pp. 365–382.

43 S. Pakrashy, P. K. Mandal, S. K. Dey, S. M. Choudhury, F. A. Alasmary, A. S. Almalki, M. A. Islam and M. Dolai, *ACS omega*, 2022, **7**, 33408–33422.

44 B. Das, S. Pakrashy, G. C. Das, U. Das, F. A. Alasmary, S. M. Wabaidur, M. A. Islam and M. Dolai, *J. Fluoresc.*, 2022, **32**, 1263–1277.

45 F. C. Hay and L. Hudson, *Practical Immunology [by] Leslie Hudson [and] Frank C Hay*, Blackwell Scientific Pub, 1989.

46 B. Das, K. C. Murmu, S. K. Dey, S. M. Chaudhuri, Z. M. Almarhoon, M. Z. Ansari, P. P. Bag and M. Dolai, *Inorg. Chem. Commun.*, 2024, **170**, 113108.

47 W. Yang, X. Chen, H. Su, W. Fang and Y. Zhang, *Chem. Commun.*, 2015, **51**, 9616–9619.

48 D. Udhayakumari, S. Naha and S. Velmathi, *Anal. Methods*, 2017, **9**, 552–578.

49 (a) A. Cuervo, P. D. Dans, J. L. Carrascosa, and L. Fumagalli, Proc. Natl. Acad. Sci., 2014, 111, 3624-3630. (b) J. Eden, P. R. C. Gascoyne, R. Pethig, J. Chem. Soc. Faraday Trans.,1980, 76, 426–434.

View Article Online
DOI: 10.1039/D5AY00778J

- The data supporting this article have been included as part of the Supplementary Information.